JACS
JOURNAL OF THE AMERICAN CHEMICAL SOCIETY
pubs.acs.org/JACS
Article

Doubly Threaded Slide-Ring Polycatenane Networks

Laura F. Hart, William R. Lenart, Jerald E. Hertzog, Jongwon Oh, Wilson R. Turner, Joseph M. Dennis, and Stuart J. Rowan*

Cite This: https://doi.org/10.1021/jacs.3c02837
Read Online

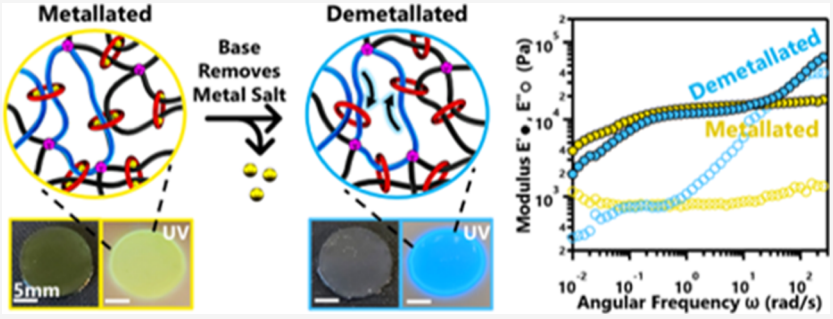

ABSTRACT: Crosslinking in polymer networks leads to intrinsic structural inhomogeneities that result in brittle materials. Replacing fixed covalent crosslinks with mobile ones in mechanically interlocked polymers (MIPs), such as in slide-ring networks (SRNs) in which interlocked crosslinks are formed when polymer chains are threaded through crosslinked rings, can lead to tougher, more robust networks. An alternative class of MIPs is the polycatenane network (PCN), in which the covalent crosslinks are replaced with interlocked rings that introduce the unusual catenane's mobility elements (elongation, rotation, and twisting) as connections between polymer chains. A slide-ring polycatenane network (SR-PCN), with doubly threaded rings embedded as crosslinks in a covalent network, combines the mobility features of both the SRNs and PCNs, where the catenated ring crosslinks can slide along the polymer backbone between the two limits of network bonding (covalent and interlocked). This work explores using a metal ion-templated doubly threaded pseudo[3]rotaxane (P3R) crosslinker, combined with a covalent crosslinker and a chain extender, to access such networks. A catalyst-free nitrile-oxide/alkyne cycloaddition polymerization was used to vary the ratio of P3R and covalent crosslinker to yield a series of SR-PCNs that vary in the amount of interlocked crosslinking units. Studies on their mechanical properties show that metal ions fix the rings in the network, leading to similar behavior as the covalent PEG gels. Removal of the metal ion frees the rings resulting in a high-frequency transition attributed to the additional relaxation of polymer chains through the catenated rings while also increasing the rate of poroelastic draining at longer timescales.

■ INTRODUCTION

The mobility and subsequent relaxations of polymer chains between crosslinks in networks often dictate many of the material's properties, such as modulus, elasticity, creep rate, stress relaxation, and impact mitigation.[1−3] However, kinetic limitations during network formation introduce topological defects, such as loops and dangling ends, reducing the number of elastically effective chains and producing a weaker and softer material. In addition, inhomogeneous distributions of covalent crosslinks lead to stress localization and brittle behavior (Figure 1a).[2−4] Over the years, many different approaches have been taken to improve the mechanical behavior and energy dissipation of polymer networks and gels.[3,5,6] A structural approach to this is a double-network gel (a class of interpenetrating networks),[7] which exhibits impressive enhancements in mechanical properties. It has been shown that the toughening mechanism in such gels relies on the different properties of the two or more networks that are partially interlocked on a molecular scale but not covalently bonded.

Interpenetrating networks are one class of mechanically interlocked polymers (MIPs),[6] which consist of non-covalently bonded components held together by mechanical bonds. Another class of MIPs is the slide-ring network (SRN), a subset of polyrotaxane[8] materials where polymer threaded rings are the crosslinking units within the polymer network. One method of accessing SRNs is by covalently crosslinking the rings on polyrotaxanes to form mobile figure-of-eight crosslinks (Figure 1b).[9−15] The sliding motion of the rings along the polymer chain allows these mobile crosslinks to adjust during applied loads, which can result in a range of

Received: March 18, 2023

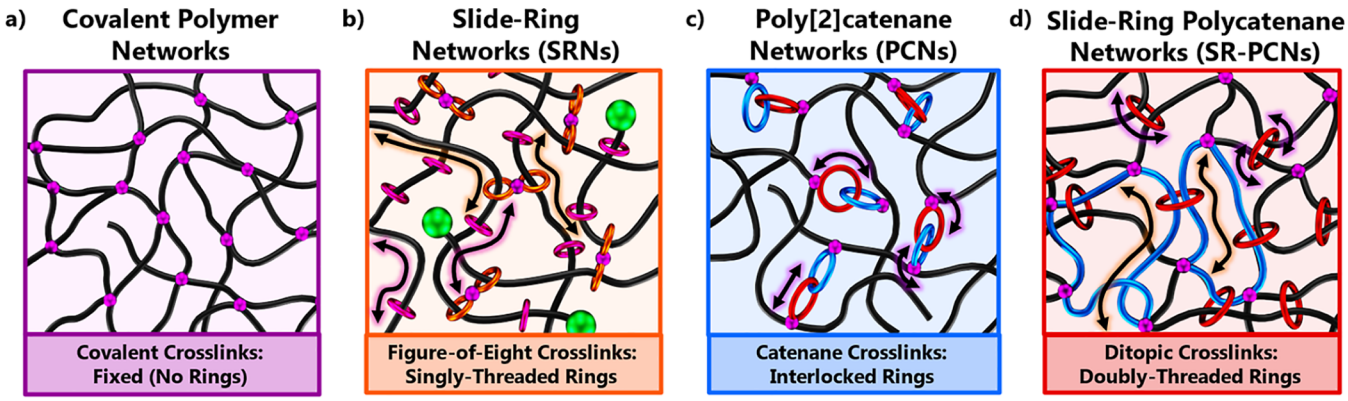

Figure 1. Schematics of covalent and selected MIP networks. (a) Fixed crosslinking in the covalent polymer network leads to an inhomogeneous distribution of covalent crosslinks (purple), where the shortest chains break under deformation. (b) A SRN comprised figure-of-eight crosslinks (orange rings) and singly threaded rings (pink) that can slide along polymer chains (arrows) but cannot dethread in the presence of stoppers (green). (c) A PCN with [2]catenane crosslinks that impart mobility elements, such as elongation, rotation, and twisting (arrows), to the networks. (d) SR-PCNs consisting of doubly threaded rings (red) embedded into covalent gels. The catenated crosslink, comprising the red ring and the (highlighted) blue chains in the network, can rotate, twist, and slide along chains (arrows) between covalent crosslinks.

interesting mechanical properties that include improved ductility and fracture behavior,[16−18] frequency-dependent relaxations,[11−15] isotropic chain deformation during elongation,[19] and suppressed stretch-induced swelling.[20] The most studied class of such materials are cyclodextrin (CD)-based SRNs, and these materials have been explored in applications such as vibration- and sound-dampening insulation,[21] superabsorbent materials,[22] elastic binders for Li-ion battery anodes,[23] coatings for anti-fouling applications,[21,24] and a wide selection of self-healing[25−28] and stimuli-responsive systems.[29−32]

Polycatenane networks (PCNs),[33−36] polymers that contain interlocked rings, are a less developed class of MIP networks that utilize mechanical bonding between two or more interlocked rings (macrocycles) within the polymer architecture.[6] The presence of elastically active concatenated rings in elastomers without covalent crosslinks[37] provides the basis for an elastic response, suggesting that incorporating cyclic components can influence material properties through the motion of interlocked rings in the network. Figure 1c is a schematic of a poly[2]catenane network in which the crosslinking unit is a [2]catenane (two interlocked rings) moiety.[35,36] The presence of these [2]catenane crosslinks imbues the networks with increased mobility derived from the elongation, rotation, and twisting (arrows, Figure 1c) of the interlocked rings relative to the same network without the catenane moieties. As with the SRNs, the mobility elements introduced by the nature of the interlocked architecture impact the properties of the network. For example, controlling the mobility of the interlocked crosslinks in the poly[2]catenane networks through metallation/demetallation[36] or intercomponent hydrogen bonding[35] leads to mechanically adaptive networks that can reversibly switch between rigid and flexible states. [2]Catenanes can also serve as mechanical protecting groups to divert tensional forces away from mechanically active functional groups in actuating polymers.[38]

Of course, SRNs and PCNs have very different types of mobility elements. The most apparent difference between the two is the translational motion of the ring along the polymer backbone in the SRNs (the magnitude of which depends on the total length of the polymer chain and the number of rings threaded onto the polymer).[6,39] Conceptually, combining elements of these two types of networks within a single crosslink moiety produces a different class of MIP where doubly threaded ring crosslinks can slide along the network backbone as well as rotate and twist (i.e., as is depicted in Figure 1d). Furthermore, changing the crosslink topology should influence the coupled network relaxations between ring mobility and chain diffusion[40] and potentially impact other properties such as solvent transport through the network during deformation.

MIP networks that only contain doubly threaded rings are less explored as synthetic access to such materials is not well developed.[41] Early studies of SRNs with doubly threaded rotaxane moieties as the crosslinker leveraged γ-CD as the ring, but the cavity size of CDs and the solvent interactions that drive complex formation limit the variety of polymers available as the threading component.[42−44] Previous attempts with template-directed assembly of doubly threaded rings have shown that low-quality gels form when the rings remain bound to the chain and ring dethreading limits practical utility. Rather than inserting a stopper after polymerization to prevent dethreading, this work shows doubly threaded rings are maintained in a network by incorporating a tetrafunctional pseudo[3]rotaxane (P3R) crosslinker into the synthesis of a crosslinked PEG-based network. A key aspect here is that a percolating covalent network is maintained to prevent/limit dethreading, and a goal of this work was to examine if the replacement of a small percentage ($\leq$30%) of the covalent crosslinks with interlocked crosslinks influences the mechanical properties of these networks. Such networks, called here slide-ring polycatenane networks (SR-PCNs, Figure 1d), were targeted by copolymerizing varying amounts of a tetrafunctional P3R with a tetrafunctional PEG-based crosslinker and an appropriate ditopic monomer. The result is a gel with large catenated crosslinks, where one ring component is the doubly threaded ring, and the other ring components are formed by the polymer network (blue chains in Figure 1d). The incorporation of these interlocked moieties into a covalent network introduces a new frequency-dependent relaxation into the PEG gel, while also drastically increasing the rate of poroelastic draining.

https://doi.org/10.1021/jacs.3c02837
J. Am. Chem. Soc. XXXX, XXX, XXX−XXX

RESULTS AND DISCUSSION

Synthesis of SR-PCNs. In targeting the SR-PCNs, a doubly threaded pseudo[3]rotaxane (P3R) moiety that is stable under the network reaction conditions is required. Metal ion templating is a common route to interlocked molecules, and many different ligands and metal ion combinations have been used to form interlocked compounds under different reaction conditions.[45−47] Recently, the terdentate 2,6-bis(*N*-alkyl-benzimidazolyl)pyridine (Bip)[48,49] ligand and its derivatives have been used to build doubly threaded mechanically interlocked compounds, such as poly[*n*]catenanes[50−52] and [3]rotaxanes.[53] Building on this prior work, the Bip-containing ditopic macrocycle **1** and bis-alkyne thread component **2** were synthesized from their corresponding bis-phenolic Bip derivatives[48,50] via Williamson ether synthesis (Schemes S1 and S2). The ditopic macrocycle incorporates two Bip ligands joined by rigid naphthalene linkers that prevent both ligands in the ring from binding to the same Zn^{2+} ion.[53] As such, the most thermodynamically favorable way for these ligands to form 2:1 Bip/metal complexes is by forming the doubly threaded P3R complex [**1:2$_2$:Zn(II)$_2$**, Figure 2a]. A solution of $Zn(NTf_2)_2$ is titrated into a 2:1 mixture of the ditopic macrocycle **1** and bis-alkyne thread **2** and monitored via ^{1}H-NMR to achieve the stoichiometry required for the P3R formation (Scheme S3 and Figure S1). The template-directed assembly of the desired P3R complex (with no observable pseudo[2]rotaxane) was confirmed by the downfield shift of the aromatic Bip protons on **1** and **2** in the NMR spectrum after adding 2 equiv of Zn^{2+} (Figure S2).

With the P3R complex as a suitable doubly threaded crosslinking moiety, the next step was to find reaction conditions that minimized its dethreading during network formation while maximizing the incorporation of macrocycle **1** into the network. The catalyst-free nitrile-oxide/alkyne click[54−58] reaction was chosen as the network-forming reaction because it should allow access to the SR-PCN gels by simply mixing the components in solution. This click reaction has been shown by Takata to be useful in the synthesis of low-molecular-weight rotaxanes,[59,60] main-chain poly[2]rotaxanes, and poly[3]rotaxanes.[61] Reaction of the tetra-alkyne end-capped 4-arm poly(ethylene glycol) (4-arm PEG-alkyne) (**4**, M_n = 5 kg mol^{-1}) and the difunctional nitrile-oxide monomer[62] **3** yields the covalent gel **5$_{96}$** with a high gel fraction (GF, determined gravimetrically, eq S1)[63] of >96% (number subscript refers to the GF of the covalent gel) confirming the overall suitability of the nitrile-oxide/alkyne click reaction. A series of SR-PCNs that vary in the amount of catenane crosslinks was accessed by reacting the difunctional nitrile-oxide monomer **3** with different ratios of the P3R crosslinker [**1:2$_2$:Zn(II)$_2$**] and **4** (keeping the [nitrile-oxide]/[alkyne] ratio 1:1) (Figure 2a).

A two-step, one-pot reaction was utilized to access the SR-PCNs (Figure 2a and Scheme S4). The P3R crosslinker [**1:2$_2$:Zn(II)$_2$**] was initially reacted with a large excess of a difunctional nitrile-oxide monomer **3** for 4 h (the total amount of **3** is kept constant regardless of P3R crosslinker content) before sufficient 4-arm PEG-alkyne crosslinker (**4**) was added to balance the stoichiometric ratio between alkyne and nitrile-oxide. The resulting SR-PCNs (**6$_{X/Y}$**) were prepared with varying amounts of P3R crosslinker, where *X* and *Y* are the molar percentage of **4** and **1:2$_2$:Zn(II)$_2$** crosslinkers used in the network synthesis, respectively. The gels were washed by heating in chloroform (~5 mL/mg of dry sample) for 4 h to remove any low-molecular-weight components. After washing, the metallated SR-PCNs (**6$_{X/YM}$**) (Figure 2b) have a light

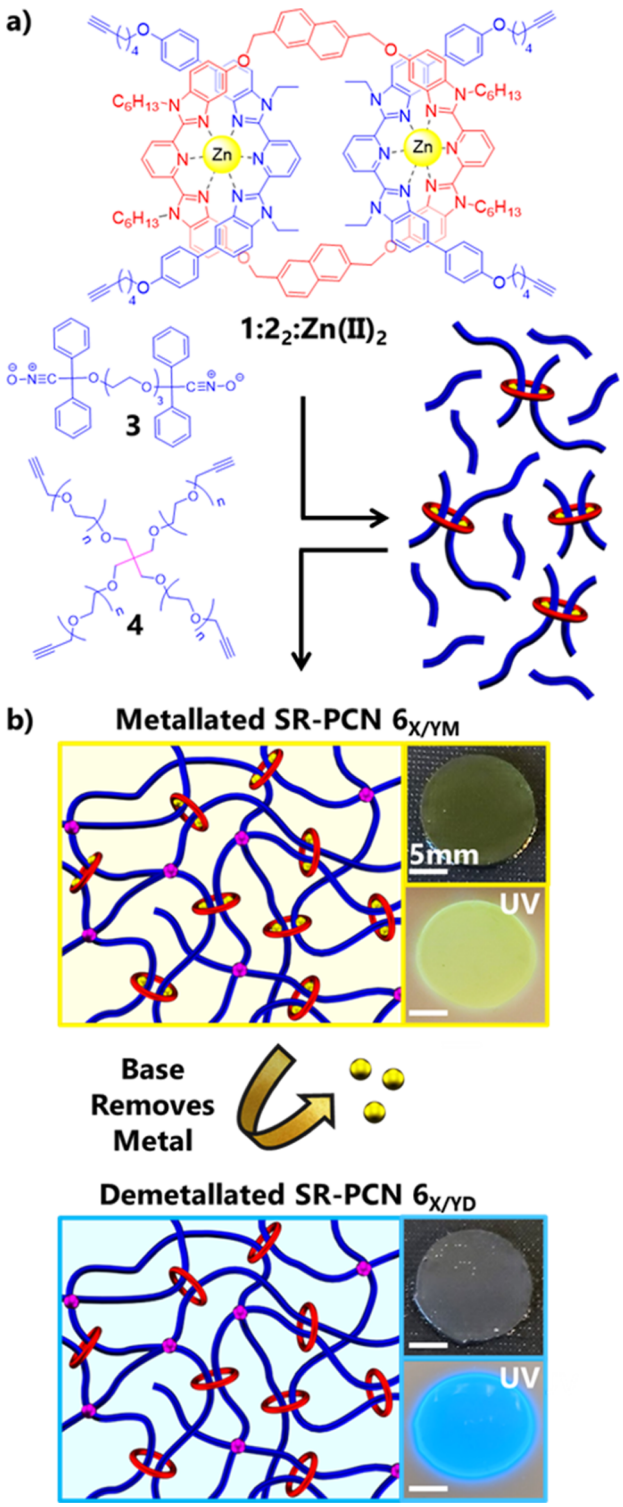

Figure 2. (a) Two-step reaction of tetra-alkyne pseudo[3]rotaxane crosslinker **1:2$_2$:Zn(II)$_2$** (*Y* = 0−30 mol %) with nitrile-oxide monomer **3** and a 4-arm PEG-alkyne **4** (*X* = 100−*Y* mol %) to yield the metallated gels (**6$_{X/YM}$**) with varying amounts of fixed and metallated ring crosslinks. (b) Treating **6$_{X/YM}$** with a dilute solution of base (tetrabutylammonium hydroxide, TBAOH) removes Zn^{2+} ions from the network, causing an observable change in color under visible and 365 nm UV light (**6$_{80/20M}$** and **6$_{80/20D}$** pictured, 5 mm scale bar).

https://doi.org/10.1021/jacs.3c02837
J. Am. Chem. Soc. XXXX, XXX, XXX−XXX

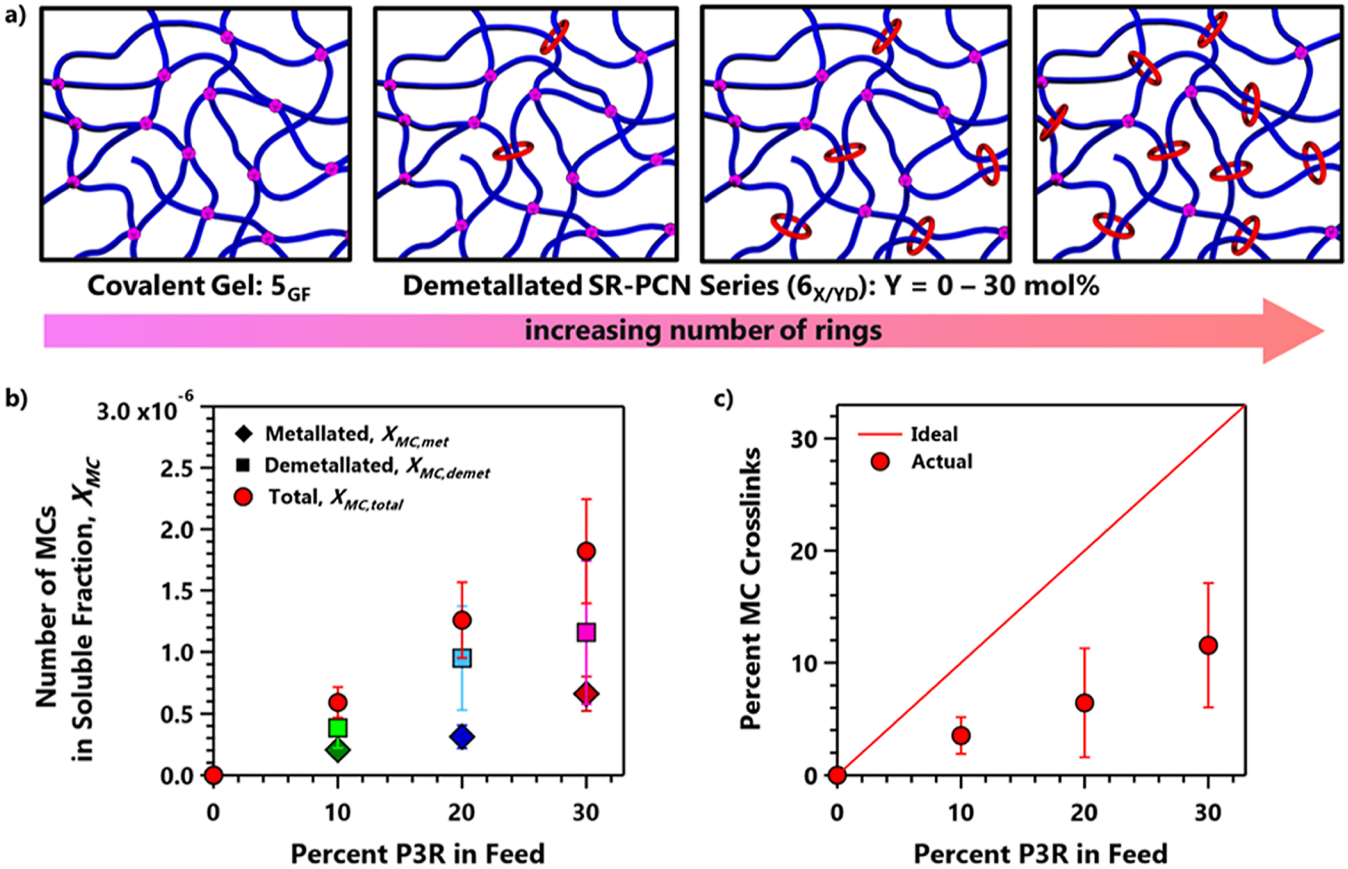

Figure 3. (a) Schematic of a covalent gel ($\mathbf{5}_{GF}$) and demetallated SR-PCNs ($\mathbf{6}_{X/YD}$) with an increasing number of doubly threaded rings (Y = 0−30 mol %). (b) The average number (moles) of macrocycle (MC) in the metallated ($X_{MC,met}$, diamonds; $\mathbf{6}_{90/10M}$ green, $\mathbf{6}_{80/20M}$ blue, $\mathbf{6}_{70/30M}$ dark red), and demetallated ($X_{MC,demet}$, squares; $\mathbf{6}_{90/10D}$ light green, $\mathbf{6}_{80/20D}$ light blue, and $\mathbf{6}_{70/30D}$ pink) soluble fractions determined from ^{1}H NMR experiments and eq S3. The total number of MC in the soluble fraction ($X_{MC,total}$) is plotted in red (circles). (c) The percent of MC crosslinks in the network, calculated from eq S7, plotted against the percent of total crosslinker in the feed that is P3R (100 × [**1**:$\mathbf{2}_2$:Zn(II)$_2$]/([**1**:$\mathbf{2}_2$:Zn(II)$_2$] + [**4**])) content. The ideal percent of MC crosslinks (solid red line), assuming 100% incorporation based on the crosslinker feed ratio, is plotted for comparison.

yellow color, and exhibit a yellow fluorescence under 365 nm UV light originating from the Bip/Zn^{2+} complexes[51] and qualitatively confirms the successful incorporation of the P3R crosslinker into the network. Base treatment of the metallated SR-PCNs, utilizing a dilute solution of tetrabutylammonium hydroxide (TBAOH), is accompanied by a shift in the UV−vis spectra (Figure S3) and a change in the color of the material under visible and UV light (Figure 2b). The demetallated gels ($\mathbf{6}_{X/YD}$) were washed repeatedly to ensure the complete extraction of metal salts and any soluble fractions (including rings) not connected to the network structure.

Controlling the monomer composition in this reaction provided a series of SR-PCNs ($\mathbf{6}_{90/10}$, $\mathbf{6}_{80/20}$, and $\mathbf{6}_{70/30}$) with an increasing number of doubly threaded rings (Y = 0−30 mol %; Figure 3a). ^{1}H NMR studies were (see the Supporting Information for experimental details) used to determine the amount of macrocycle (MC) retained in the network by measuring the number (moles) of MC in the demetallated soluble fractions (Figures S4 and S5). Perhaps not surprisingly, the total amount of free macrocycle **1** obtained in the soluble fraction, X_{MC} (mol) calculated from eq S3, increases with the amount of P3R crosslinker used in the synthesis (Figure 3b, red circles). However, importantly for this study, the percent of MC (**1**) crosslinks that remain in the SR-PCN (calculated from eq S7) increases with the increase in fraction of P3R crosslinker used in the polymerization (Figure 3c).

The successful incorporation of the rings is further confirmed by thermal gravimetric analysis (TGA) studies of the dry demetallated SR-PCNs, which show an increase in the residual mass as the amount of macrocycle **1** is increased in the synthesis (Figure S6), consistent with the increased incorporation of more aromatic rings in these networks. Furthermore, differential scanning calorimetry (DSC) thermograms of both the metallated and demetallated (dry) SR-PCNs reveal a reduction in the PEG crystallinity as the relative amount of 4-arm PEG-alkyne crosslinker is reduced with the addition of more P3R crosslinker (Table S3). While these data confirm the incorporation of the rings into the network it is not able to confirm that all the rings are doubly threaded. It is certainly possible that a small percentage of these rings are singly threaded, especially in gels synthesized with a higher amount of P3R.

It is important to note that the introduction of the P3R crosslinker into the synthesis results in a drop in the overall SR-PCN gel fraction (GF, wt %, eq S1) based on the weight of the (dry) demetallated SR-PCN after washing and the original weight of the (dry) metallated SR-PCN after gelation (Figure S8, squares). Therefore, in addition to the covalent gel $\mathbf{5}_{96}$ (with a GF of 96%) two covalent networks ($\mathbf{5}_{GF}$) were

https://doi.org/10.1021/jacs.3c02837
J. Am. Chem. Soc. XXXX, XXX, XXX−XXX

prepared at different reaction times which resulted in gel fractions of 86% ($\mathbf{5}_{86}$, 24 h) and 74% ($\mathbf{5}_{74}$, 12 h) to provide GFs similar to $\mathbf{6}_{X/YM}$ and $\mathbf{6}_{X/YD}$ for better comparison (Figure S8, purple circles). Swelling studies show that the average weight-based swelling ratios for $\mathbf{6}_{X/YM}$ and $\mathbf{6}_{X/YD}$ (eq S10)[64] in *N*-methyl-2-pyrrolidone (NMP) are relatively similar to the covalent control $\mathbf{5}_{74}$ (Figure S10). Therefore, all gels were swollen to approximately the same extent over 24 h before mechanical testing.

Relationship between Macrocycle Content and SR-PCN Mechanical Properties. With a series of SR-PCNs in hand, the next goal was to explore the influence of the ring crosslinks on the gels' mechanical properties. The metallated gels were included in this investigation to determine if replacing a covalent crosslink with a ring crosslink influences the material properties while in the bound state, and to help separate and aid the comparison of the demetallated SR-PCNs to covalent controls. To this end, compressive stress relaxation experiments were carried out on the NMP swollen SR-PCNs ($\mathbf{6}_{90/10M}$, $\mathbf{6}_{80/20M}$, and $\mathbf{6}_{70/30M}$) and the two covalent networks with comparable GF ($\mathbf{5}_{86}$ and $\mathbf{5}_{74}$). The long relaxation time of the swollen covalent gels, measured under compression, generally corresponds to the poroelastic relaxation of the solvent draining from the network.[65−67] The rate of this draining is related to the viscosity of the fluid and the average mesh size of the network, defined as the linear distance between two adjacent crosslinks.[68,69] Generally, in a system with fixed crosslinks, there is a distribution of mesh sizes that dictates fluid draining, and the corresponding distribution of relaxation times can be described with a stretched exponential function (eq 1)[70]

$$E(t)/E_0 = \exp(-(t/\tau)^{\beta}) \quad (1)$$

where $E(t)$ is the modulus at time t, E_0 is the initial modulus at time zero, $E(t = 0)/E_0 = 1$ after normalization, τ is the relaxation time, and β ($0 \leq \beta \leq 1$) is the stretching parameter that captures a distribution in relaxation time (Table S4). In both the covalent controls $\mathbf{5}_{GF}$ and metallated SR-PCNs $\mathbf{6}_{X/YM}$, the stretched exponential fits well (dashed lines, Figure 4a), indicating that a single relaxation distribution governs the poroelastic relaxation process in these gels. By normalizing the relaxation time (taken when $E(t) = 1/e$) of the catenated gels to covalent controls of equivalent GF (Figure S11), it is possible to estimate the contribution of the MC content to this relaxation time. Incorporating the metallated ring crosslinks substantially decreases the relaxation time relative to the equivalent covalent gel of similar GF, increasing solvent draining.

After demetallating these three SR-PCNs with base to yield $\mathbf{6}_{90/10D}$, $\mathbf{6}_{80/20D}$, and $\mathbf{6}_{70/30D}$, there is a substantial decrease in the long relaxation time of the gels, with a decrease of about an order of magnitude for the gels with the highest MC content (Figure 4b,c). The relaxation times of the SR-PCNs, when normalized by the relaxation time of a covalent gel with equivalent GF (Figure S11), are much smaller than one, indicating there are other contributions to the decrease in relaxation time beyond GF. A possible explanation for this effect is that the incorporation of the mobile crosslinks results in an adaptable mesh size as the rings can slide to accommodate the stress on the network, facilitating faster flow of the solvent. Another indication of the ring crosslink mobility in the network is the failure of a single stretched exponential to fully capture the poroelastic relaxation time.

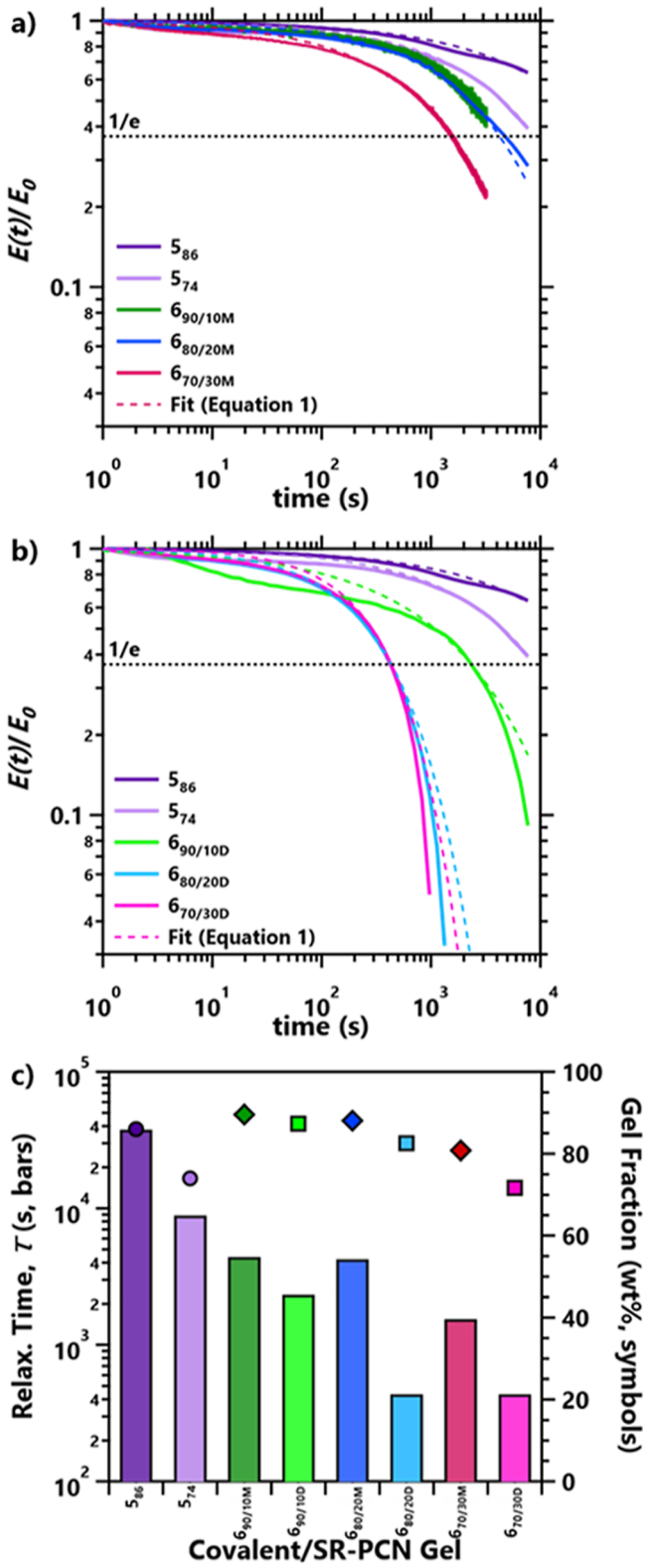

Figure 4. (a) Overlay of the normalized stress relaxation moduli, $E(t)/E_0$, for the metallated SR-PCNs ($\mathbf{6}_{90/10M}$ green, $\mathbf{6}_{80/20M}$ blue, and $\mathbf{6}_{70/30M}$ red) swollen in NMP (including the covalent controls: $\mathbf{5}_{86}$ dark purple and $\mathbf{5}_{74}$ light purple). (b) $E(t)/E_0$ overlay for the demetallated SR-PCNs ($\mathbf{6}_{90/10D}$ light green, $\mathbf{6}_{80/20D}$ light blue, and $\mathbf{6}_{70/30D}$ pink), highlighting the failure of the stretched exponential (eq 1, dashed lines) to capture the changes in the relaxation behavior. The dashed line at $E(t) = 1/e$ determined the relaxation time, τ (s). (c) Comparison of τ (on a log scale) for all gels (bars) shows a significant

https://doi.org/10.1021/jacs.3c02837
J. Am. Chem. Soc. XXXX, XXX, XXX−XXX

Figure 4. continued

decrease in estimated τ for $\mathbf{6}_{X/YD}$ irrespective of the decrease in GF (symbols, calculated from eq S1).

While a single stretched exponential function can capture a single relaxation event with a distribution of times, the dynamic nature of the mesh size distributions and the mobility of the rings themselves likely impact the poroelastic relaxation times, suggesting convolution of relaxation phenomena in the network. Previous quasi-elastic[71] and inelastic[72] neutron scattering studies on CD-SRNs suggest that when the rings are well dispersed, the timescale for ring sliding is slow and on the order of the poroelastic relaxation seen in this system. An additive model (eq S11) might be expected to fit if the measurement of these relaxations do not interact, usually when the relaxation timescale is significantly different. Using this model, leaving the relaxation times unbound and the stretching parameters bound between 0 and 1, gives a better fit to the experimental data; however, it still fails to accurately capture the behavior of the curve (Figure S12). If the relaxation events interact (e.g., through energy transfer), then a product model could better capture the relaxation times.[73] The simplest way to model this interaction would be the product of the two exponential decays from the same initial stress (eq S12). This fit was performed with the same parameter bounds as the additive model (Figure S12) but also failed to capture the stress relaxation of the of PC-SRNs. The interaction of ring sliding with poroelastic draining is clearly more complex than these three simple models can account for.

To further probe the properties of these SR-PCNs, small-amplitude oscillatory compression (SAOC) studies were performed to explore the frequency-dependent mechanical response as well as the faster relaxation process. Figure 5 summarizes the frequency dependence of the storage modulus E' and tan δ of metallated and demetallated SR-PCNs swollen in NMP (loss modulus E'' is provided in Figure S13). The storage moduli of the covalent control and metallated samples display minimal frequency dependence above 1 rad/s. While below this frequency, a typical poroelastic behavior is observed wherein the modulus decreases with the frequency because of solvent draining from the network[74] (Figure 5a).

Demetallation resulted in an additional higher-frequency relaxation observed as an increase in the storage modulus with frequency (Figure 5b) and peak in the tan δ (Figures 5c and S14). Using the frequency at the peak intensity of the tan δ, a characteristic relaxation time of 50 and 16 ms was estimated for the $\mathbf{6}_{90/10D}$ and $\mathbf{6}_{80/20D}$, respectively. While the peak of the tan δ for the $\mathbf{6}_{70/30D}$ is beyond the limits of the instrument, the onset of a relaxation is observed at the higher frequencies and suggests this sample would continue the trend of a decreasing characteristic relaxation time. Rationalized as a change in network mobility, this faster relaxation occurs as mobile ring crosslinks replace the covalent crosslinks. Interestingly, as this ring relaxation is traversed from low to high frequencies, the sliding appears to become restrained and behaves similarly to an entrapped entanglement resulting in a higher concentration of elastically effective chains in the network and a higher modulus than the covalent control of similar GF.[75] Similar to the stress relaxation studies, as the ring content increases, a number of complex catenated structures can form and contribute to the relaxation behavior in convoluted ways. However, the data suggest that the slower relaxation is likely

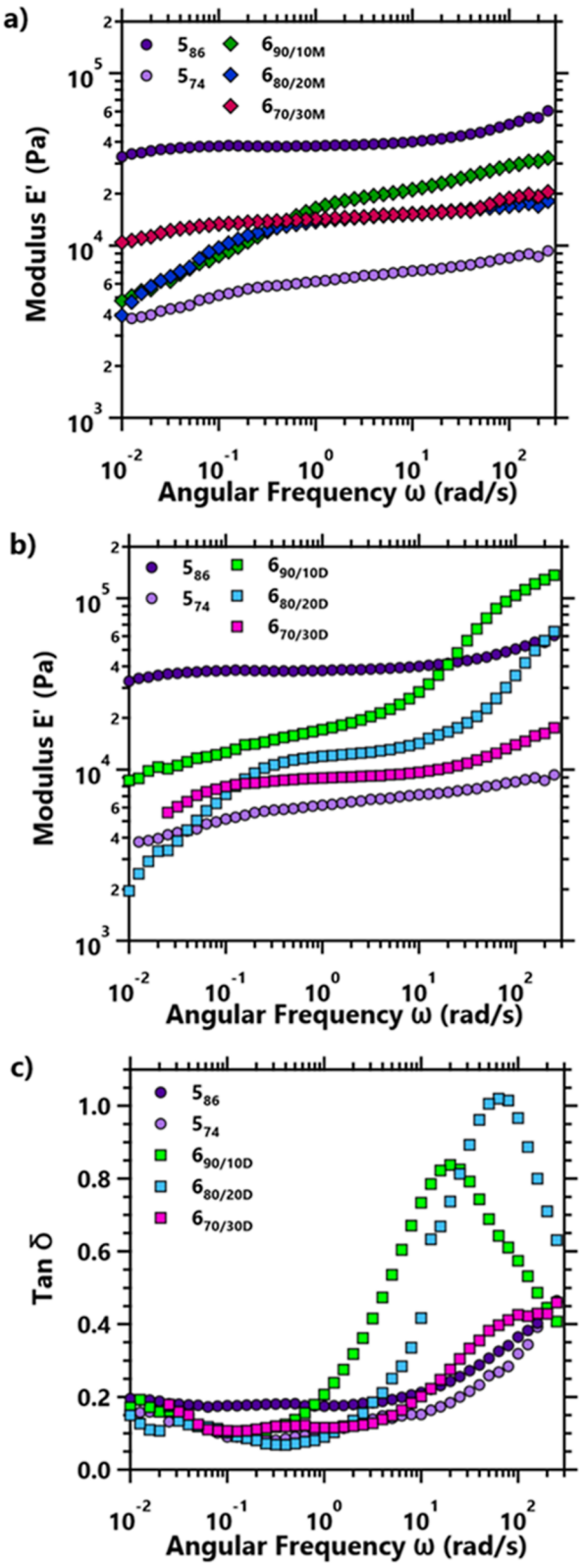

Figure 5. Small-amplitude oscillatory compression (SAOC) frequency sweeps for (a) covalent ($\mathbf{5}_{86}$, dark purple; $\mathbf{5}_{74}$, light purple), metallated (diamonds) SR-PCNs ($\mathbf{6}_{90/10M}$, green; $\mathbf{6}_{80/20M}$, blue; $\mathbf{6}_{70/30M}$, red), and (b) demetallated (squares) SR-PCNs ($\mathbf{6}_{90/10D}$, light green; $\mathbf{6}_{80/20D}$, light blue; and $\mathbf{6}_{70/30D}$, pink) swollen in NMP. (c) Tan δ vs angular frequency for covalent and demetallated NMP gels. Samples were preloaded with 0.025 N to ensure uniform contact between the sample and plates. Frequency sweeps were performed from 1000 to 0.01 rad/s with a strain amplitude of 1%.

https://doi.org/10.1021/jacs.3c02837
J. Am. Chem. Soc. XXXX, XXX, XXX−XXX

related to ring diffusion along the chain, while the faster relaxation is related to the reptation-like diffusion of the chain through the ring.[13,71,76] Harnessing the variety of relaxations available in SR-PCNs could prove valuable in a range of advanced applications, such as impact mitigation.

■ CONCLUSIONS

Catalyst-free NOAC polymerization of a tetra-alkyne pseudo[3]rotaxane and a tetra-alkyne covalent crosslinker with a difunctional nitrile-oxide monomer can be used to synthesize SR-PCNs with varying amounts of interlocked and covalent crosslinks. Incorporating metallated ring crosslinks into a PEG gel hastens the slow poroelastic relaxation behavior seen in the stress relaxation studies. At higher strain rates, the metallated gel behaves similarly to the covalent controls, indicating that the metallated rings act as fixed crosslinks at fast timescales. Demetallation frees the catenated rings to move in the system providing new avenues of mechanical relaxation showing similar behavior to a glass transition in the storage modulus and tan δ, while the time for poroelastic draining rapidly decreases. Copolymerization of doubly threaded pseudo[3]rotaxanes and covalent crosslinkers offers a simple way to include complex catenane moieties into a network structure and provides a versatile platform for deeper investigations of the structure−property relationships [such as the effect of (i) molecular weight between crosslinks, (ii) sterics of thread component, (iii) ring size, (iv) nature of the solvent, (v) (partial) remetallation of the gels, and (vi) addition of different metal ions, to name few] in these SR-PCNs.

■ ASSOCIATED CONTENT

Supporting Information

The Supporting Information is available free of charge at https://pubs.acs.org/doi/10.1021/jacs.3c02837.

Full experimental details and characterization of **1** and **2**, assembly of **1:2$_2$:Zn(II)$_2$**, gel preparation and characterization including UV−vis, ^{1}H-NMR studies on soluble fractions, thermal properties, gel fraction calculations, swelling ratio (wt %), compressive stress relaxation, and SAOC rheology experiments (PDF)

■ AUTHOR INFORMATION

Corresponding Author

Stuart J. Rowan − *Pritzker School of Molecular Engineering, University of Chicago, Chicago, Illinois 60637, United States; Department of Chemistry, University of Chicago, Chicago, Illinois 60637, United States; Chemical Science and Engineering Division and Center for Molecular Engineering, Argonne National Laboratory, Lemont, Illinois 60434, United States;* orcid.org/0000-0001-8176-0594; Email: stuartrowan@uchicago.edu

Authors

Laura F. Hart − *Pritzker School of Molecular Engineering, University of Chicago, Chicago, Illinois 60637, United States;* orcid.org/0000-0001-7908-9332

William R. Lenart − *Pritzker School of Molecular Engineering, University of Chicago, Chicago, Illinois 60637, United States;* orcid.org/0000-0002-3660-256X

Jerald E. Hertzog − *Pritzker School of Molecular Engineering, University of Chicago, Chicago, Illinois 60637, United States; Department of Chemistry, University of Chicago, Chicago, Illinois 60637, United States;* orcid.org/0000-0002-9692-7331

Jongwon Oh − *Pritzker School of Molecular Engineering, University of Chicago, Chicago, Illinois 60637, United States;* orcid.org/0000-0002-9690-7613

Wilson R. Turner − *Pritzker School of Molecular Engineering, University of Chicago, Chicago, Illinois 60637, United States; Department of Chemistry, University of Chicago, Chicago, Illinois 60637, United States*

Joseph M. Dennis − *Polymers Branch, Sciences of Extreme Materials Division, U.S. DEVCOM Army Research Laboratory, Aberdeen Proving Grounds, Maryland 21005, United States*

Complete contact information is available at: https://pubs.acs.org/10.1021/jacs.3c02837

Author Contributions

All authors discussed and commented on the manuscript.

Notes

The authors declare no competing financial interest.

■ ACKNOWLEDGMENTS

This work was funded by National Science Foundation (NSF) grant number CHE-1903603. Research was also sponsored in part by the Army Research Laboratory and was accomplished under Cooperative agreement number W911NF-20-2-0044. The views and conclusions contained in this document are those of the authors and should not be interpreted as representing the official policies, either expressed or implied, of the Army Research Laboratory, or the U.S. Government. The U.S. Government is authorized to reproduce and distribute reprints for Government purposes notwithstanding any copyright notation herein. This work made use of the shared facilities at the University of Chicago Materials Research Science and Engineering Center (MRSEC) and the Soft Matter Characterization Facility (SMCF), which are supported by National Science Foundation under award number DMR-2011854. We would like to thank the director of this facility, Dr. Philip Griffin, for assistance with thermal and mechanical characterization.

■ ABBREVIATIONS

SRN	slide-ring network
MIP	mechanically interlocked polymer
PCN	polycatenane network
SR-PCN	slide-ring polycatenane network
P3R	pseudo[3]rotaxane
PEG	poly(ethylene glycol)
CD	cyclodextrin
NOAC	nitrile-oxide/alkyne cycloaddition
GF	gel fraction
NMP	*N*-methyl-2-pyrrolidone
SAOC	small-amplitude oscillatory compression

■ REFERENCES

(1) Whittaker, A. K. The Structure of Polymer Networks. In *Modern Magnetic Resonance*; Webb, G. A., Ed.; Springer Netherlands: Dordrecht, 2006; pp 583−589.

(2) Zhong, M.; Wang, R.; Kawamoto, K.; Olsen, B. D.; Johnson, J. A. Quantifying the Impact of Molecular Defects on Polymer Network Elasticity. *Science* **2016**, *353*, 1264−1268.

(3) Gu, Y.; Zhao, J.; Johnson, J. A. A (Macro)Molecular-Level Understanding of Polymer Network Topology. *Trends Chem.* **2019**, *1*, 318−334.
(4) *Polymer Networks: Principles of Their Formation, Structure and Properties*; Stepto, R. F., Ed.; Springer Netherlands, 1998.
(5) Shibayama, M. Structure-Mechanical Property Relationship of Tough Hydrogels. *Soft Matter* **2012**, *8*, 8030−8038.
(6) Hart, L. F.; Hertzog, J. E.; Rauscher, P. M.; Rawe, B. W.; Tranquilli, M. M.; Rowan, S. J. Material Properties and Applications of Mechanically Interlocked Polymers. *Nat. Rev. Mater.* **2021**, *6*, 508−530.
(7) Gong, J. P. Why Are Double Network Hydrogels so Tough? *Soft Matter* **2010**, *6*, 2583−2590.
(8) Chen, L.; Sheng, X.; Li, G.; Huang, F. Mechanically Interlocked Polymers Based on Rotaxanes. *Chem. Soc. Rev.* **2022**, *51*, 7046−7065.
(9) Okumura, Y.; Ito, K. The Polyrotaxane Gel: A Topological Gel by Figure-of-Eight Cross-Links. *Adv. Mater.* **2001**, *13*, 485−487.
(10) Mayumi, K.; Ito, K.; Kato, K.; Mayumi, K. *Polyrotaxane and Slide-Ring Materials; Monographs in Supramolecular Chemistry*; Royal Society of Chemistry: Cambridge, 2015.
(11) Fleury, G.; Schlatter, G.; Brochon, C.; Travelet, C.; Lapp, A.; Lindner, P.; Hadziioannou, G. Topological Polymer Networks with Sliding Cross-Link Points: The "Sliding Gels". Relationship between Their Molecular Structure and the Viscoelastic as Well as the Swelling Properties. *Macromolecules* **2007**, *40*, 535−543.
(12) Kato, K.; Ito, K. Dynamic Transition between Rubber and Sliding States Attributed to Slidable Cross-Links. *Soft Matter* **2011**, *7*, 8737−8740.
(13) Kato, K.; Yasuda, T.; Ito, K. Viscoelastic Properties of Slide-Ring Gels Reflecting Sliding Dynamics of Partial Chains and Entropy of Ring Components. *Macromolecules* **2013**, *46*, 310−316.
(14) Fleury, G.; Schlatter, G.; Brochon, C.; Hadziioannou, G. Unveiling the Sliding Motion in Topological Networks: Influence of the Swelling Solvent on the Relaxation Dynamics. *Adv. Mater.* **2006**, *18*, 2847−2851.
(15) Kato, K.; Karube, K.; Nakamura, N.; Ito, K. The Effect of Ring Size on the Mechanical Relaxation Dynamics of Polyrotaxane Gels. *Polym. Chem.* **2015**, *6*, 2241−2248.
(16) Liu, C.; Kadono, H.; Yokoyama, H.; Mayumi, K.; Ito, K. Crack Propagation Resistance of Slide-Ring Gels. *Polymer* **2019**, *181*, 121782.
(17) Liu, C.; Kadono, H.; Mayumi, K.; Kato, K.; Yokoyama, H.; Ito, K. Unusual Fracture Behavior of Slide-Ring Gels with Movable Cross-Links. *ACS Macro Lett.* **2017**, *6*, 1409−1413.
(18) Liu, C.; Mayumi, K.; Hayashi, K.; Jiang, L.; Yokoyama, H.; Ito, K. Direct Observation of Large Deformation and Fracture Behavior at the Crack Tip of Slide-Ring Gel. *J. Electrochem. Soc.* **2019**, *166*, B3143−B3147.
(19) Shinohara, Y.; Kayashima, K.; Okumura, Y.; Zhao, C.; Ito, K.; Amemiya, Y. Small-Angle X-Ray Scattering Study of the Pulley Effect of Slide-Ring Gels. *Macromolecules* **2006**, *39*, 7386−7391.
(20) Konda, A.; Mayumi, K.; Urayama, K.; Takigawa, T.; Ito, K. Influence of Structural Characteristics on Stretching-Driven Swelling of Polyrotaxane Gels with Movable Cross Links. *Macromolecules* **2012**, *45*, 6733−6740.
(21) Noda, Y.; Hayashi, Y.; Ito, K. From Topological Gels to Slide-ring Materials. *J. Appl. Polym. Sci.* **2014**, *131*, 40509.
(22) Pang, C.; Wang, H.; Zhang, F.; Patel, A. K.; Lee, H. P.; Wooley, K. L. Glucose-derived Superabsorbent Hydrogel Materials Based on Mechanically-interlocked Slide-ring and Triblock Copolymer Topologies. *J. Polym. Sci.* **2023**, *61*, 937−950.
(23) Choi, S.; Kwon, T.; Coskun, A.; Choi, J. W. Highly Elastic Binders Integrating Polyrotaxanes for Silicon Microparticle Anodes in Lithium Ion Batteries. *Science* **2017**, *357*, 279−283.
(24) Zhuo, Y.; Li, T.; Wang, F.; Hakonsen, V.; Xiao, S.; He, J.; Zhang, Z. An Ultra-Durable Icephobic Coating by a Molecular Pulley. *Soft Matter* **2019**, *15*, 3607−3611.
(25) Nakahata, M.; Mori, S.; Takashima, Y.; Yamaguchi, H.; Harada, A. Self-Healing Materials Formed by Cross-Linked Polyrotaxanes with Reversible Bonds. *Chem* **2016**, *1*, 766−775.
(26) De Bo, G. Combining Mobile and Dynamic Bonds for Rapid and Efficient Self-Healing Materials. *Chem* **2016**, *1*, 672−673.
(27) Cho, I. S.; Ooya, T. Cell-Encapsulating Hydrogel Puzzle: Polyrotaxane-Based Self-Healing Hydrogels. *Chem.—Eur. J.* **2020**, *26*, 913−920.
(28) Kobayashi, Y.; Zheng, Y.; Takashima, Y.; Yamaguchi, H.; Harada, A. Physical and Adhesion Properties of Supramolecular Hydrogels Cross-Linked by Movable Cross-Linking Molecule and Host-Guest Interactions. *Chem. Lett.* **2018**, *47*, 1387−1390.
(29) Sakai, T.; Murayama, H.; Nagano, S.; Takeoka, Y.; Kidowaki, M.; Ito, K.; Seki, T. Photoresponsive Slide-Ring Gel. *Adv. Mater.* **2007**, *19*, 2023−2025.
(30) Bin Imran, A.; Esaki, K.; Gotoh, H.; Seki, T.; Ito, K.; Sakai, Y.; Takeoka, Y. Extremely Stretchable Thermosensitive Hydrogels by Introducing Slide-Ring Polyrotaxane Cross-Linkers and Ionic Groups into the Polymer Network. *Nat. Commun.* **2014**, *5*, 5124.
(31) Yasumoto, A.; Gotoh, H.; Gotoh, Y.; Imran, A. B.; Hara, M.; Seki, T.; Sakai, Y.; Ito, K.; Takeoka, Y. Highly Responsive Hydrogel Prepared Using Poly(N-Isopropylacrylamide)-Grafted Polyrotaxane as a Building Block Designed by Reversible Deactivation Radical Polymerization and Click Chemistry. *Macromolecules* **2017**, *50*, 364−374.
(32) Ma, W.; Fang, H.; Tian, D.; Zheng, L.; Xie, M.; Sun, R. Solvent-Free Stretchable Photo-Responsive Supramolecular Actuator Topologically Cross-Linked by Azobenzene-Cyclodextrin Based Slide-Ring System. *Dyes Pigm.* **2022**, *200*, 110120.
(33) Zhang, K.; Lackey, M. A.; Cui, J.; Tew, G. N. Gels Based on Cyclic Polymers. *J. Am. Chem. Soc.* **2011**, *133*, 4140−4148.
(34) Oike, H.; Mouri, T.; Tezuka, Y. A Cyclic Macromonomer Designed for a Novel Polymer Network Architecture Having Both Covalent and Physical Linkages. *Macromolecules* **2001**, *34*, 6229−6234.
(35) Xing, H.; Li, Z.; Wu, Z. L.; Huang, F. Catenane Crosslinked Mechanically Adaptive Polymer Gel. *Macromol. Rapid Commun.* **2018**, *39*, 1700361−1700366.
(36) Nosiglia, M. A.; Colley, N. D.; Danielson, M. K.; Palmquist, M. S.; Delawder, A. O.; Tran, S. L.; Harlan, G. H.; Barnes, J. C. Metalation/Demetalation as a Postgelation Strategy To Tune the Mechanical Properties of Catenane-Crosslinked Gels. *J. Am. Chem. Soc.* **2022**, *144*, 9990−9996.
(37) Hu, P.; Madsen, J.; Huang, Q.; Skov, A. L. Elastomers without Covalent Cross-Linking: Concatenated Rings Giving Rise to Elasticity. *ACS Macro Lett.* **2020**, *9*, 1458−1463.
(38) Zhang, M.; De Bo, G. A Catenane as a Mechanical Protecting Group. *J. Am. Chem. Soc.* **2020**, *142*, 5029−5033.
(39) Jiang, L.; Liu, C.; Mayumi, K.; Kato, K.; Yokoyama, H.; Ito, K. Highly Stretchable and Instantly Recoverable Slide-Ring Gels Consisting of Enzymatically Synthesized Polyrotaxane with Low Host Coverage. *Chem. Mater.* **2018**, *30*, 5013−5019.
(40) Xing, Z.; Shu, D. W.; Lu, H.; Fu, Y. Q. Untangling the Mechanics of Entanglements in Slide-Ring Gels towards Both Super-Deformability and Toughness. *Soft Matter* **2022**, *18*, 1302−1309.
(41) Yamamoto, K.; Nameki, R.; Sogawa, H.; Takata, T. Macrocyclic Dinuclear Palladium Complex as a Novel Doubly Threaded [3]Rotaxane Scaffold and Its Application as a Rotaxane Cross-Linker. *Angew. Chem., Int. Ed.* **2020**, *59*, 18023−18028.
(42) Jang, K.; Iijima, K.; Koyama, Y.; Uchida, S.; Asai, S.; Takata, T. Synthesis and Properties of Rotaxane-Cross-Linked Polymers Using a Double-Stranded γ-CD-Based Inclusion Complex as a Supramolecular Cross-Linker. *Polymer* **2017**, *128*, 379−385.
(43) Iijima, K.; Aoki, D.; Otsuka, H.; Takata, T. Synthesis of Rotaxane Cross-Linked Polymers with Supramolecular Cross-Linkers Based on γ-CD and PTHF Macromonomers: The Effect of the Macromonomer Structure on the Polymer Properties. *Polymer* **2017**, *128*, 392−396.

https://doi.org/10.1021/jacs.3c02837
J. Am. Chem. Soc. XXXX, XXX, XXX−XXX

(44) Harada, A. Design and Construction of Supramolecular Architectures Consisting of Cyclodextrins and Polymers. *Metal Complex Catalysts Supercritical Fluid Polymerization Supramolecular Architecture*; Springer Berlin Heidelberg: Berlin, Heidelberg, 2017; pp 141−191.

(45) Lewis, J. E. M.; Beer, P. D.; Loeb, S. J.; Goldup, S. M. Metal Ions in the Synthesis of Interlocked Molecules and Materials. *Chem. Soc. Rev.* **2017**, *46*, 2577−2591.

(46) Denis, M.; Goldup, S. M. The Active Template Approach to Interlocked Molecules. *Nat. Rev. Chem.* **2017**, *1*, 0061.

(47) Hubin, T. J.; Busch, D. H. Template Routes to Interlocked Molecular Structures and Orderly Molecular Entanglements. *Coord. Chem. Rev.* **2000**, *200−202*, 5−52.

(48) McKenzie, B. M.; Miller, A. K.; Wojtecki, R. J.; Johnson, J. C.; Burke, K. A.; Tzeng, K. A.; Mather, P. T.; Rowan, S. J. Improved Synthesis of Functionalized Mesogenic 2,6-Bisbenzimidazolylpyridine Ligands. *Tetrahedron* **2008**, *64*, 8488−8495.

(49) Piguet, C.; Bernardinelli, G.; Williams, A. F.; Bocquet, B. Formation of the First Isomeric [2]Catenates by Self-Assembly about Two Different Metal Ions. *Angew. Chem., Int. Ed.* **1995**, *34*, 582−584.

(50) Wojtecki, R. J.; Wu, Q.; Johnson, J. C.; Ray, D. G.; Korley, L. T. J.; Rowan, S. J. Optimizing the Formation of 2,6-Bis(N-Alkyl-Benzimidazolyl)Pyridine-Containing [3]Catenates through Component Design. *Chem. Sci.* **2013**, *4*, 4440−4448.

(51) Wu, Q.; Rauscher, P. M.; Lang, X.; Wojtecki, R. J.; De Pablo, J. J.; Hore, M. J. A.; Rowan, S. J. Poly[n]Catenanes: Synthesis of Molecular Interlocked Chains. *Science* **2017**, *358*, 1434−1439.

(52) Tranquilli, M. M.; Wu, Q.; Rowan, S. J. Effect of Metallosupramolecular Polymer Concentration on the Synthesis of Poly[n]Catenanes. *Chem. Sci.* **2021**, *12*, 8722−8730.

(53) Hertzog, J. E.; Maddi, V. J.; Hart, L. F.; Rawe, B. W.; Rauscher, P. M.; Herbert, K. M.; Bruckner, E. P.; de Pablo, J. J.; Rowan, S. J. Metastable Doubly Threaded [3]Rotaxanes with a Large Macrocycle. *Chem. Sci.* **2022**, *13*, 5333−5344.

(54) Lee, Y. G.; Yonekawa, M.; Koyama, Y.; Takata, T. Synthesis of a Kinetically Stabilized Homoditopic Nitrile N-Oxide Directed toward Catalyst-Free Click Polymerization. *Chem. Lett.* **2010**, *39*, 420−421.

(55) Sogawa, H.; Monjiyama, S.; Wang, C.-G.; Tsutsuba, T.; Takata, T. New Synthetic Route to OH-Functionalized Nitrile N -Oxide and Polyfunctional Nitrile N -Oxides for Click Crosslinking and Decrosslinking of Natural Rubber. *Polym. Chem.* **2018**, *9*, 4382−4385.

(56) Wang, C. G.; Koyama, Y.; Yonekawa, M.; Uchida, S.; Takata, T. Polymer Nitrile N-Oxides Directed toward Catalyst- and Solvent-Free Click Grafting. *Chem. Commun.* **2013**, *49*, 7723−7725.

(57) Tsutsuba, T.; Sogawa, H.; Takata, T. Preparation of a Highly Reactive Polymer Click Reagent, PEG Nitrile N-Oxide, and Its Application in Block and Star Polymer Synthesis. *Polym. Chem.* **2017**, *8*, 1445−1448.

(58) Singh, I.; Zarafshani, Z.; Lutz, J.-F.; Heaney, F. Metal-Free "Click" Chemistry: Efficient Polymer Modification via 1,3-Dipolar Cycloaddition of Nitrile Oxides and Alkynes. *Macromolecules* **2009**, *42*, 5411−5413.

(59) Matsumura, T.; Ishiwari, F.; Koyama, Y.; Takata, T. C−C Bond-Forming Click Synthesis of Rotaxanes Exploiting Nitrile N -Oxide. *Org. Lett.* **2010**, *12*, 3828−3831.

(60) Yuki, T.; Koyama, Y.; Matsumura, T.; Takata, T. Click Annulation of Pseudo[2]Rotaxane to [2]Catenane Exploiting Homoditopic Nitrile N -Oxide. *Org. Lett.* **2013**, *15*, 4438−4441.

(61) Lee, Y.-G.; Koyama, Y.; Yonekawa, M.; Takata, T. Synthesis of Main-Chain-Type Polyrotaxanes by New Click Polymerization Using Homoditopic Nitrile N -Oxides via Rotaxanation−Polymerization Protocol. *Macromolecules* **2010**, *43*, 4070−4080.

(62) Tsutsuba, T.; Sogawa, H.; Kuwata, S.; Takata, T. Kinetically Stabilized Aliphatic Nitrile N-Oxides as Click Agents: Synthesis, Structure, and Reactivity. *Chem. Lett.* **2017**, *46*, 315−318.

(63) Ahmad, Z.; Salman, S.; Khan, S. A.; Amin, A.; Rahman, Z. U.; Al-Ghamdi, Y. O.; Akhtar, K.; Bakhsh, E. M.; Khan, S. B. Versatility of Hydrogels: From Synthetic Strategies, Classification, and Properties to Biomedical Applications. *Gels* **2022**, *8*, 167.

(64) Zhang, K.; Feng, W.; Jin, C. Protocol Efficiently Measuring the Swelling Rate of Hydrogels. *MethodsX* **2020**, *7*, 100779.

(65) Dey, K.; Agnelli, S.; Borsani, E.; Sartore, L. Degradation-Dependent Stress Relaxing Semi-Interpenetrating Networks of Hydroxyethyl Cellulose in Gelatin-PEG Hydrogel with Good Mechanical Stability and Reversibility. *Gels* **2021**, *7*, 277.

(66) Chan, E. P.; Deeyaa, B.; Johnson, P. M.; Stafford, C. M. Poroelastic Relaxation of Polymer-Loaded Hydrogels. *Soft Matter* **2012**, *8*, 8234−8240.

(67) Wijesinghe, A. M.; Kingsbury, H. B. On the Dynamic Behavior of Poroelastic Materials. *J. Acoust. Soc. Am.* **1979**, *65*, 90−95.

(68) Cuccia, N. L.; Pothineni, S.; Wu, B.; Méndez Harper, J.; Burton, J. C. Pore-Size Dependence and Slow Relaxation of Hydrogel Friction on Smooth Surfaces. *Proc. Natl. Acad. Sci. U.S.A.* **2020**, *117*, 11247−11256.

(69) Peppas, N. A.; Bures, P.; Leobandung, W.; Ichikawa, H. Hydrogels in Pharmaceutical Formulations. *Eur. J. Pharm. Biopharm.* **2000**, *50*, 27−46.

(70) Kuang, X.; Liu, G.; Dong, X.; Wang, D. Correlation between Stress Relaxation Dynamics and Thermochemistry for Covalent Adaptive Networks Polymers. *Mater. Chem. Front.* **2017**, *1*, 111−118.

(71) Yasuda, Y.; Hidaka, Y.; Mayumi, K.; Yamada, T.; Fujimoto, K.; Okazaki, S.; Yokoyama, H.; Ito, K. Molecular Dynamics of Polyrotaxane in Solution Investigated by Quasi-Elastic Neutron Scattering and Molecular Dynamics Simulation: Sliding Motion of Rings on Polymer. *J. Am. Chem. Soc.* **2019**, *141*, 9655−9663.

(72) Mayumi, K.; Nagao, M.; Endo, H.; Osaka, N.; Shibayama, M.; Ito, K. Dynamics of Polyrotaxane Investigated by Neutron Spin Echo. *Phys. B* **2009**, *404*, 2600−2602.

(73) Berberan-Santos, M. N.; Bodunov, E. N.; Valeur, B. Mathematical Functions for the Analysis of Luminescence Decays with Underlying Distributions 1. Kohlrausch Decay Function (Stretched Exponential). *Chem. Phys.* **2005**, *315*, 171−182.

(74) Galli, M.; Comley, K. S. C.; Shean, T. A. V.; Oyen, M. L. Viscoelastic and Poroelastic Mechanical Characterization of Hydrated Gels. *J. Mater. Res.* **2009**, *24*, 973−979.

(75) Syed, I. H.; Stratmann, P.; Hempel, G.; Klüppel, M.; Saalwächter, K. Entanglements, Defects, and Inhomogeneities in Nitrile Butadiene Rubbers: Macroscopic versus Microscopic Properties. *Macromolecules* **2016**, *49*, 9004−9016.

(76) Mayumi, K.; Ito, K. Structure and Dynamics of Polyrotaxane and Slide-Ring Materials. *Polymer* **2010**, *51*, 959−967.

https://doi.org/10.1021/jacs.3c02837
J. Am. Chem. Soc. XXXX, XXX, XXX−XXX